Geophysical Research Letters

Supporting Information for

Coastal Mountains Amplified the Impacts of Orbital Forcing on East Asian Climate in the Late Cretaceous

Jian Zhang[1], Sascha Flögel[2], Yongyun Hu[1], Anni Zhao[1], Runjian Chu[3], Chenguang Zhu[4], and Chengshan Wang[3]

[1]Department of Atmospheric and Oceanic Sciences, School of Physics, Peking University, Beijing, China.

[2]GEOMAR Helmholtz Centre for Ocean Research Kiel, Kiel, Germany.

[3]State Key Laboratory of Biogeology and Environmental Geology, China University of Geosciences Beijing, Beijing, China.

[4]Department of Atmospheric Science, School of Environmental Studies, China University of Geosciences, Wuhan, China.

Contents of this file

Text S1. Paleogeography and Paleovegetation

Paleogeography (Figure S1a) and paleovegetation (Figure S1b) of ~90 Ma modified from Sewall et al. (2007) are used in this study. Following the manual provided by NCAR (Rosenbloom et al., 2011), the topography and bathymetry were smoothed and the mid-ocean ridges were removed to get rid of the singularity. Some very small land patches are removed, and a small land area (~170 °E-170°W) was added around the paleo-Arctic Ocean. Based on Liu et al (2013), these modifications have little influence on surface climate, but can help alleviate convergence difficulties of the ocean.

Text S2. Description for detailed setting of modeling experiments

CFCs concentrations are set to 0, and CH_4 and N_2O are set to 760 ppbv and 270 ppbv, respectively. All other atmospheric constituents including O_3 and aerosols are set to preindustrial levels, i.e. the default values of the CESM1.2.2. Although CO_2 concentration during the Cretaceous could have varied greatly (Bice and Norris, 2002; Huber et al., 2002; Wang et al., 2014), it has been shown that the Asian climate during the Cretaceous was not sensitive to changes in pCO_2 (Farnsworth et al., 2019; Zhang et al., 2019). We use a relatively high value of 1120 ppmv, which is close to reconstructed values for the early Late Cretaceous (Foster et al., 2017).

The three coupled experiments are run for 3000 model years in order for the global climate to reach statistical equilibrium. The monthly sea surface temperatures (SSTs) and sea ice fractions are averaged over the last 100 years, which are used as the boundary condition for the other three uncoupled experiments in the same set. All 9 uncoupled experiments equilibrate quickly (less than a few years), so they are run for only 25 model years. The last 20 years of data were analyzed and presented in this study.

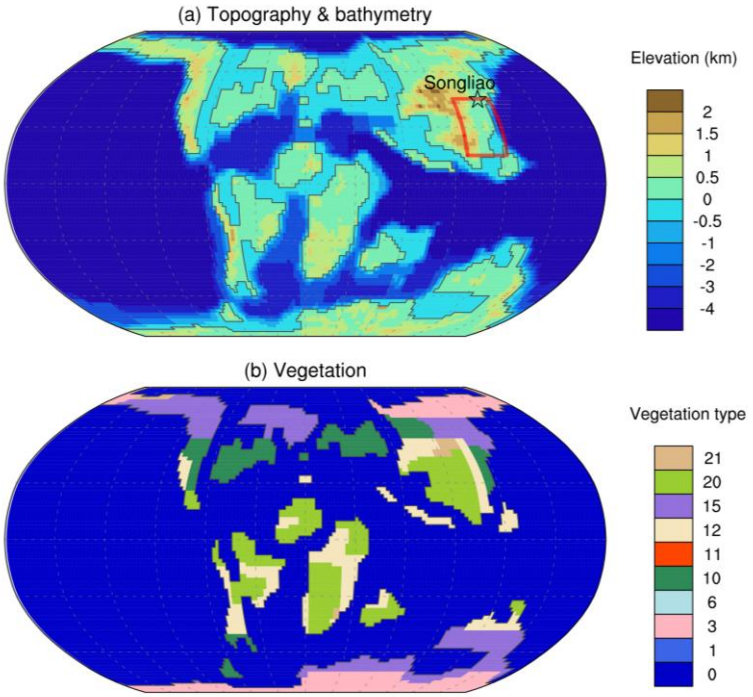

Figure S1. Paleogeogrpahy (a) and paleovegetation (b) modified from Sewall et al. (2007). In Panel b, numbers 0 is for the ocean, 1 for the land ice, 3 for the high altitude/latitude evergreen conifer closed canopy forest, 6 for the high altitude/latitude mixed forest with equal percentage broad vs needle leaf and evergreen vs deciduous, 10 for the closed canopy, broad leaved, moist evergreen forest, 11 for the closed canopy, broadleaved, dry deciduous forest, 12 for the savanna (dry, low understory with sparse broad leaved overstory), 15 for the high altitude/latitude moist, open canopy evergreen forest with shrub understory, 20 for the wet or cool shrubland (evergreen), and 21 for the dry or warm shrubland (deciduous). These are the same as the Land Surface Model (LSM) vegetation types.

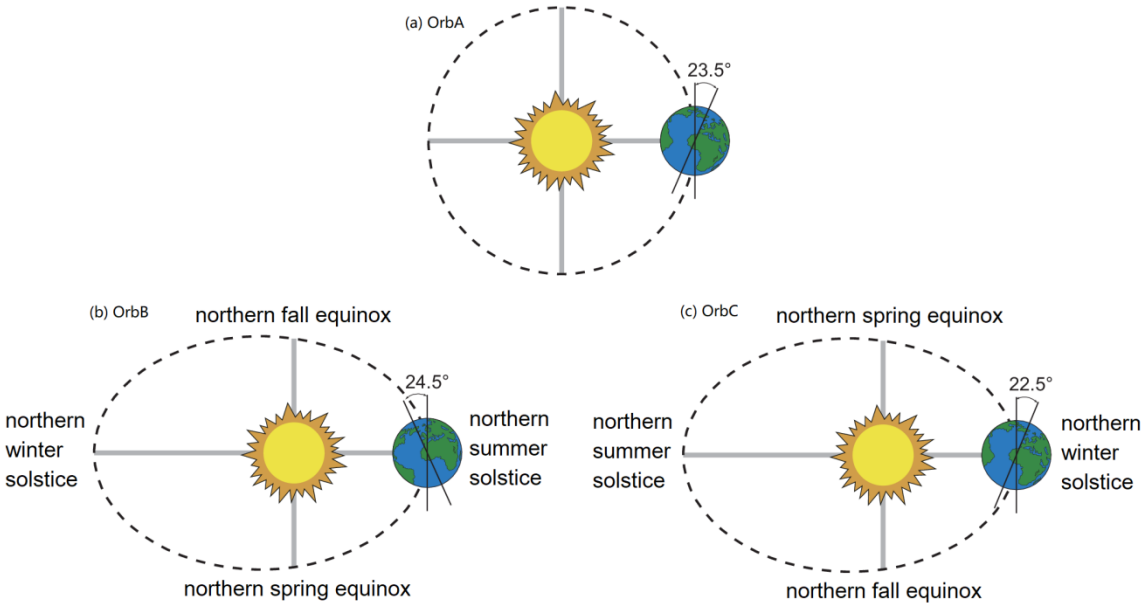

Figure S2 Orbital configurations for the control set (Set A, a) and sensitivity sets (Set B, b; and Set C, c) of experiments.

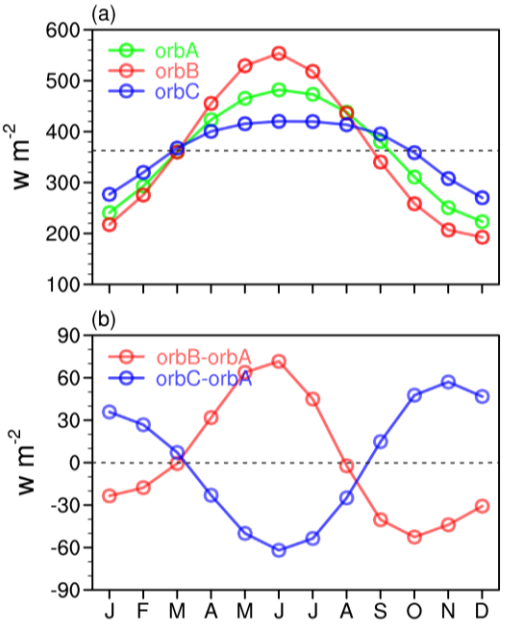

Figure S3 Annual variation in downward solar fluxes (W m^{-2}) at the top of the atmosphere averaged over latitudes 20-40 °N for different orbital configurations.

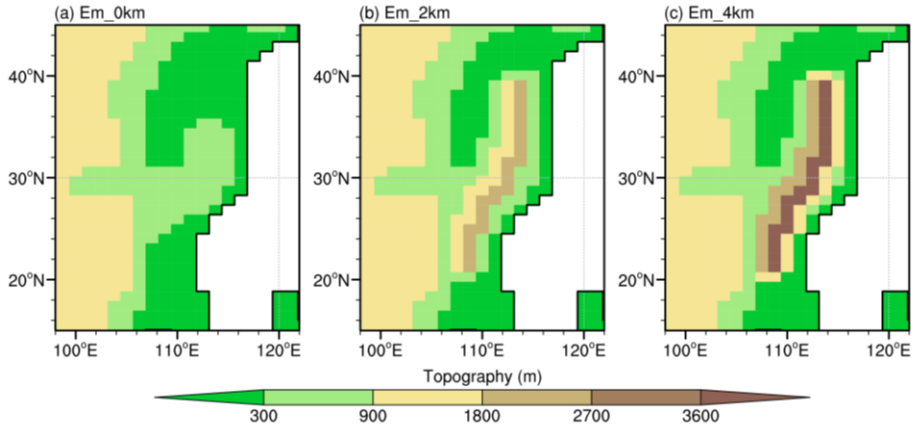

Figure S4 East Asian regional topography (the red rectangle in Figure S1a). The altitude of the coastal mountain range is 0 km (a), 2 km (b) and 4 km (c). The meridional mountain range extends from 20 ºN to 40 ºN.

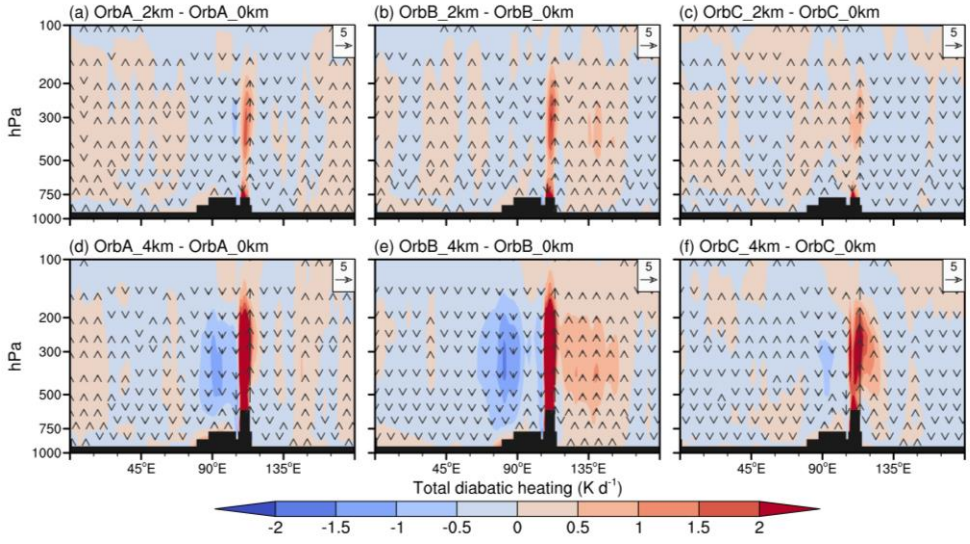

Figure S5 Zonal-vertical cross sections of total diabatic heating during summer (shaded; units: K d^{-1}) and vertical velocity (vectors; units: ×0.01 Pa s^{-1}) averaged within 20-30 °N. Top panels: differences between experiments with coastal mountains of 2 km and 0 km high. Bottom panels: differences between experiments with coastal mountains of 4 km and 0 km high. From left to right are the conditions in Set A, Set B, and SetC, respectively.

Table S1 Orbital setting and topography of experiments

Experiments	Orbital configuration	Topographical descriptions
OrbA_Cpl	Obliquity=23.5 Eccentricity=0. (Figure S2a)	Low-resolution coupled experiment without coastal mountains (Figure S1a)
OrbA_0km		High-resolution atmospheric experiment without coastal mountains (Figures S1a and S4a)
OrbA_2km		High-resolution atmospheric experiment with coastal mountains of 2 km (Figure S4b)
OrbA_4km		High-resolution atmospheric experiment with coastal mountains of 4 km (Figure S4c)
OrbB_Cpl	Obliquity=24.5, Eccentricity=0.066, Precession=270 (Figure S2b)	Same as the Experiment OrbA_Cpl
OrbB_0km		Same as the Experiment OrbA_0km
OrbB_2km		Same as the Experiment OrbA_2km
OrbB_4km		Same as the Experiment OrbA_4km
OrbC_Cpl	Obliquity=22.5, Eccentricity=0.066, Precession=90 (Figure S2c)	Same as the Experiment OrbA_Cpl
OrbC_0km		Same as the Experiment OrbA_0km
OrbC_2km		Same as the Experiment OrbA_2km
OrbC_4km		Same as the Experiment OrbA_4km

References

Bice, K.L., Norris, R.D., 2002. Possible atmospheric CO2 extremes of the Middle Cretaceous (late Albian–Turonian). Paleoceanography 17, 1070.

Farnsworth, A., Lunt, D.J., Robinson, S.A., Valdes, P.J., Roberts, W.H.G., Clift, P.D., Markwick, P., Su, T., Wrobel, N., Bragg, F., Kelland, S.-J., Pancost, R.D., 2019. Past East Asian monsoon evolution controlled by paleogeography, not CO2. Science Advances 5, 1697.

Foster, G.L., Royer, D.L., Lunt, D.J., 2017. Future climate forcing potentially without precedent in the last 420 million years. Nature communications 8, 14845.

Huber, B.T., Norris, R.D., MacLeod, K.G., 2002. Deep-sea paleotemperature record of extreme warmth during the Cretaceous. Geology 30, 123-126.

Liu, Y., Peltier, W.R., Yang, J., Vettoretti, G., 2013. The initiation of Neoproterozoic "snowball" climates in CCSM3: the influence of paleocontinental configuration. Climate of the Past 9, 2555-2577.

Rosenbloom, N., Shields, C., Brady, E., Levis, S., Yeager, S., 2011. Using CCSM3 for paleoclimate applications. National Center for Atmospheric Research.

Sewall, J.O., van de Wal, R.S.W., van der Zwan, K., van Oosterhout, C., Dijkstra, H.A., Scotese, C.R., 2007. Climate model boundary conditions for four Cretaceous time slices. Clim. Past 3, 647-657.

Wang, Y., Huang, C., Sun, B., Quan, C., Wu, J., Lin, Z., 2014. Paleo-CO2 variation trends and the Cretaceous greenhouse climate. Earth-Science Reviews 129, 136-147.

Zhang, J., Liu, Y., Fang, X., Wang, C., Yang, Y., 2019. Large dry-humid fluctuations in Asia during the Late Cretaceous due to orbital forcing: A modeling study. Palaeogeography, Palaeoclimatology, Palaeoecology 533, 109230.